S-EMG Signal Compression in One-Dimensional and Two-Dimensional Approaches

Marcel H. Trabuco, Marcus V. C. Costa, *Member, IEEE*, Bruno Macchiavello, *Member, IEEE*, and Francisco Assis de O. Nascimento, *Member, IEEE*

***Abstract*—This paper presents algorithms designed for one-dimensional (1-D) and 2-D surface electromyographic (S-EMG) signal compression. The 1-D approach is a wavelet transform based encoder applied to isometric and dynamic S-EMG signals. An adaptive estimation of the spectral shape is used to carry out dynamic bit allocation for vector quantization of transformed coefficients. Thus, an entropy coding is applied to minimize redundancy in quantized coefficient vector and to pack the data. In the 2-D approach algorithm, the isometric or dynamic S-EMG signal is properly segmented and arranged to build a 2-D representation. The high efficient video codec is used to encode the signal, using 16-bit-depth precision, all possible coding/prediction unit sizes, and all intra-coding modes. The encoders are evaluated with objective metrics, and a real signal data bank is used. Furthermore, performance comparisons are also shown in this paper, where the proposed methods have outperformed other efficient encoders reported in the literature.**

***Index Terms*—Dynamic bit allocation, HEVC encoder, S-EMG signal compression, transform-based encoder, wavelet transform.**

I. Introduction

SURFACE electromyography has been studied in several areas of human knowledge, such as clinical [1]–[3]; orthopedic and sports medicine [4], [5]; biomechanics [6]; and control systems for prostheses [7], [8]. In all the applications mentioned, one or many S-EMG channels are digitized, transmitted through a wired or wireless link to a base station, organized into a data file to be stored for offline processing, or organized in segments (sample set) for real-time applications. Each electromyographic channel is usually scanned at a rate ranging from 1 to 4 k-samples per second using two bytes to represent a sample. The A/D converters generally produce an output that varies between 12 and 16 bits [4], [6]. It is also possible to use an A/D converter with 24-bit fixed-point or floating-point word length quantization.

Manuscript received June 24, 2017; revised September 10, 2017; accepted October 16, 2017. Date of publication October 22, 2017; date of current version June 29, 2018. This work was supported in part by the National Council for Technological and Scientific Development (CNPq), a Brazilian government agency for scientific and technological development. *(Corresponding author: Francisco Assis de O. Nascimento.)*

The authors are with the University of Brasília, Brasília 70910-900, Brazil (e-mail: mhtrabuco@gmail.com; chaffim@gmail.com; bruno@cic.unb.br; assis@unb.br).

Digital Object Identifier 10.1109/JBHI.2017.2765922

The amount of bitrate generated by an experiment involving S-EMG signals must be proportional to the sampling rate, the digital word length used in quantization of the samples, the number of S-EMG channels, and the duration of the experiment. Therefore, this procedure may require a large mass memory for data storage or a high-bandwidth channel for transmission. Hence, it is important to develop coding techniques to minimize the statistical redundancy and reduce the irrelevancies in S-EMG signals. The search for efficient data compression techniques has been the focus of several studies.

Most S-EMG coding methods found in the scientific literature can be classified as either parametric coding or transform domain coding (which are normally based on the Discrete Wavelet Transform). The great majority of papers that address S-EMG parametric coding are based on Linear Predictive Coding (LPC) [9]–[14]. The LPC approach is predominantly used to represent the spectral envelope of digital signal in compressed form, and it is frequently found in speech encoders at low bit rates [15], [16]. The hybrid algorithm ACELP (Algebraic Code-Excited Linear Prediction) [16] presents good results when applied to S-EMG signals compression [12]–[14]. Compared to the transform domain methods, the LPC modeling has advantages in implementation of computational effort. However, the estimated signal spectrum is very sensitive to LPC coefficients, and the technique loses the original information in the signal phase [15]. Thus, fidelity in the decoded waveform is inferior compared to the waveform transform-based encoders. The performance of LPC encoders is limited to the theoretical limits of predictive modeling [15].

Moreover, studies considering adaptive Differential Pulse Code Modulation (ADPCM) [17], [18] applied to S-EMG compression are frequently found in the literature [19]–[22]. The real-time implementation using low computational complexity is the main improvement of this technique. Vector quantization algorithm [23] to code S-EMG time waveform is likewise found in literature [24]–[26]. The reported algorithms were designed to preserve the spectral signature of S-EMG signal to compute the main clinically interesting medical parameters, such as mean frequency and median frequency.

Waveform transform-based encoders have shown better performance evaluation based on objective metrics when compared to signal-to-noise ratio (SNR) and data compression rate [9]. Discrete Wavelet Transform (DWT) and Discrete Cosine Transform (DCT) have been applied to EMG encoders due to their energy concentration characteristic in the transformed

domain [27]. Algorithms such as embedded zero-tree wavelet (EZW) compression algorithm [28]–[30] have a high compression ratio with low distortion of the EMG waveform.

Several studies have sought to optimize the base functions to better decorrelate the S-EMG signal in the transformed domain [31]–[34]. Other researchers have invested in a hybrid approach to modify the standard transform-based encoder. For example, a vector quantization was applied on the transformed wavelet coefficient vector [35]. Another approach used mathematical models [36] or neural networks [37], [38] to approximate the spectral magnitude shape in wavelet domain. Consequently, dynamic bit allocation was carried out for quantization of wavelet-transformed coefficients.

Algorithms originally developed to compress images have also been applied to S-EMG coding [39]–[48]. In those examples, S-EMG is segmented by rectangular windows of length N (samples), and the entire signal composed of M segments is arranged into $N \times M$ matrix. Thus, two-dimensional technique is applied to code data. The use of JPEG2000 [39]–[42], [44], H.264/AVC [40], [44], HEVC [44], 2D-DCT [43], 2D-DWT [43], and 2D-fractal [45] were also reported in literature. The standard JPEG compress algorithm approach for high-density electromyography (HD EMG) was found in [46], and recurrent patterns [47] for 1D S-EMG [48] and for 2D S-EMG [44] signals were found in the literature. Furthermore, research involving compressed sensing was also encountered in the literature [49]–[53].

In this work, we present algorithms designed for 1D (one-dimensional) and 2D (two-dimensional) surface electromyographic (S-EMG) signal compression. The 1D approach is a wavelet transform-based encoder. An adaptive spectral shape estimation is used to carry out dynamic bit allocation for quantization of transformed coefficients. An entropy coding is applied to minimize redundancy in quantized coefficient vector and to pack data. In the 2D approach algorithm, the isometric or dynamic S-EMG signal are properly segmented and arranged to build a two-dimension representation. This novel 2D composition increases the spatial correlation of the signal, thereby increasing the encoding performance of a differential encoder. The H.265/HEVC encoder, a hybrid transform domain/differential encoder, is then applied. The HEVC is configured to encode the S-EMG 2D data. The encoders are evaluated with objective metrics and use a real signal data bank. Performance comparisons with other efficient encoders proposed in scientific literature are also shown.

II. 1D S-EMG Compression Algorithm

Wavelet transform based encoders with dynamic bit allocation for the transformed coefficients quantization was presented in [36]. The transformed coefficient vector, in this proposal, is quantized according to the mathematical model used for spectral shape estimation. Fig. 1 presents the proposed 1D WDAL (1D Wavelet Dynamic Adaptive-Log Bit Allocation) encoder block diagram. In this approach, the S-EMG signal is segmented into windows of length N samples. N is an integer power of 2. A discrete wavelet transform is applied to each window. The

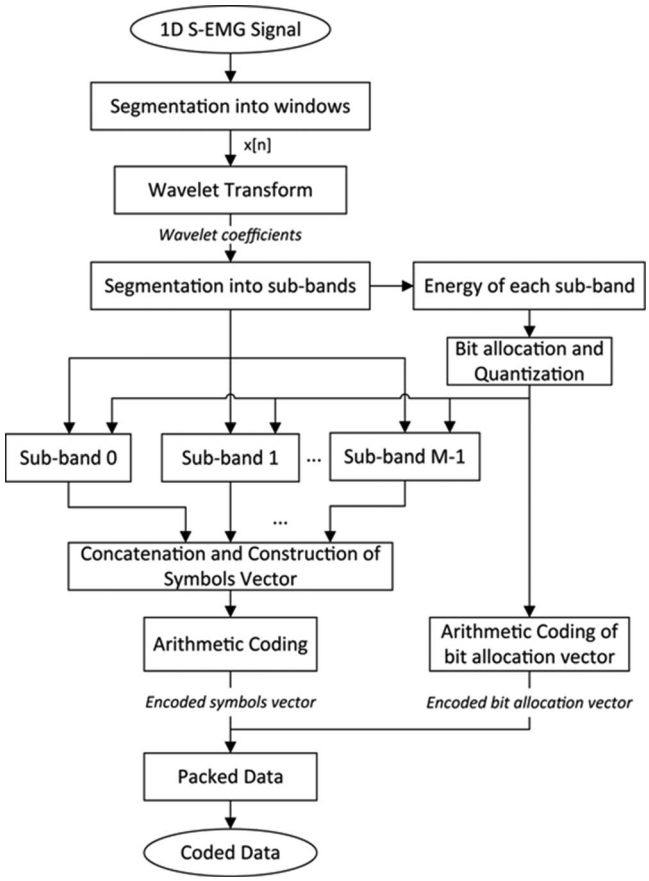

Fig. 1. Block diagram of 1D WDAL encoder.

transformed coefficient vector is segmented into sub-bands. The coefficients of each sub-band are quantized with an amount of bits indicated by the estimation model of the spectral shape. The algorithm for spectral shape estimation is adaptatively computed for each window with low-pass characteristic and leads to a bit allocation vector. This algorithm will be described below. The wavelet transform-vector quantization leads to a vector of symbols, which is compressed by a lossless compression technique. The bit allocation vector is also compressed with a lossless technique and packaged as side information. Arithmetic coding is used for lossless compression [54].

A. Spectral Shape Estimation and Transformed Vector Quantization

The dynamic range of the wavelet coefficients $W[k]$ in the transformed space is normalized to satisfy (1)

$$\max\{|W[k]|\}_{k=0,1,\ldots,N-1} \leq 2^{D-1} \tag{1}$$

where D to the word depth (in bits) with which the sequence $x[n]$ is digitalized with fixed point representation (in the cases simulated in this work, $N = 2048$ samples and $D = 16$ bits).

The transformed coefficients vector is also segmented, generating a total of M sub-bands (the examples presented in this work used $M = 16$). Each sub-band has N/M transformed coefficients (the examples presented in this work have $N/M = 128$ coefficients). For a given sub-band of index m, there are N/M

transformed coefficients that belong to the same sub-band and may be quantized up to a maximum of the word bit-depth assigned to the respective sub-band, according to the mathematical relations

$$W_q[k] = Int\left\{\frac{W[k]}{2^{D-1}}\gamma[m]\right\} \tag{2}$$

$$k = \frac{N}{M}m, \frac{N}{M}m+1, \ldots, \frac{N}{M}m+\frac{N}{M}-1 \tag{3}$$

$$\text{and } m = 0, 1, \ldots, M-1 \tag{4}$$

where $W[k]$ *and* $W_q[k]$, $k = 0, 1, \ldots, N-1$, are the original and quantized wavelet transformed coefficients, respectively. The parameter $\gamma[m]$ is obtained from an adaptive spectral shape estimator that seeks to model the S-EMG signal envelope of the spectrum energy considering that the information, although non-stationary, has a low-pass characteristic. The calculation of $\gamma[m]$ is described below.

The proposal of an adaptive model to estimate the spectral shape involves the distribution of energy in the wavelet transform domain. At this point, it is necessary to define, for a given sub-band of index m, the energy of the sub-band $E[m]$, the cumulative energy $E_a[m]$, and the vector energy of the total transformed coefficients E as

$$E[m] = \sum_{k=m\frac{N}{M}}^{(m+1)\frac{N}{M}-1} |W[k]|^2 \tag{5}$$

$$E_a[m] = \sum_{k=0}^{m} E[k] \tag{6}$$

$$E = \sum_{k=0}^{N-1} |W[k]|^2 \tag{7}$$

Based on (5)–(7), the spectral shape estimation function $\rho[m]$ is defined, which provides the amount of the total energy that has been stored up to the index m, and can be expressed as

$$\rho[m] = 1 - \frac{E_a[m-1]}{E} \; for\; m \geq 1, \quad \rho[0] = 1 \tag{8}$$

The number of bits associated to quantize the coefficients of each sub-band is computed by the expression

$$\begin{gathered} B[m] = intsup\left\{Q + \log_2(\beta\rho[m])\right\} \\ \text{if } B[m] < 0 \text{ then } B[m] = 0 \end{gathered} \tag{9}$$

where Q is a parameter in which the unit is *bits*, β is a positive scaling factor that can shift vertically the bit allocation curve, and $B[m]$ gives the maximum word bit-depth in which a coefficient of sub-band m can be quantized. Note that $B[0]$ indicates the largest bit-depth used in the quantization of the coefficient vector and is equal to

$$B[0] = intsup\{Q + \log_2(\beta)\} \tag{10}$$

For example, for $Q = 8$ bits and $\beta = Q$ chosen, lead to $B[0] = 11$ bits. A typical behavior of $B[m]$ for S-EMG signals can be illustrated as

$$\underline{B} = [11, 10, 10, 9, 9, 9, 8, 8, 8, 7, 6, 6, 4, 2, 0, 0] \tag{11}$$

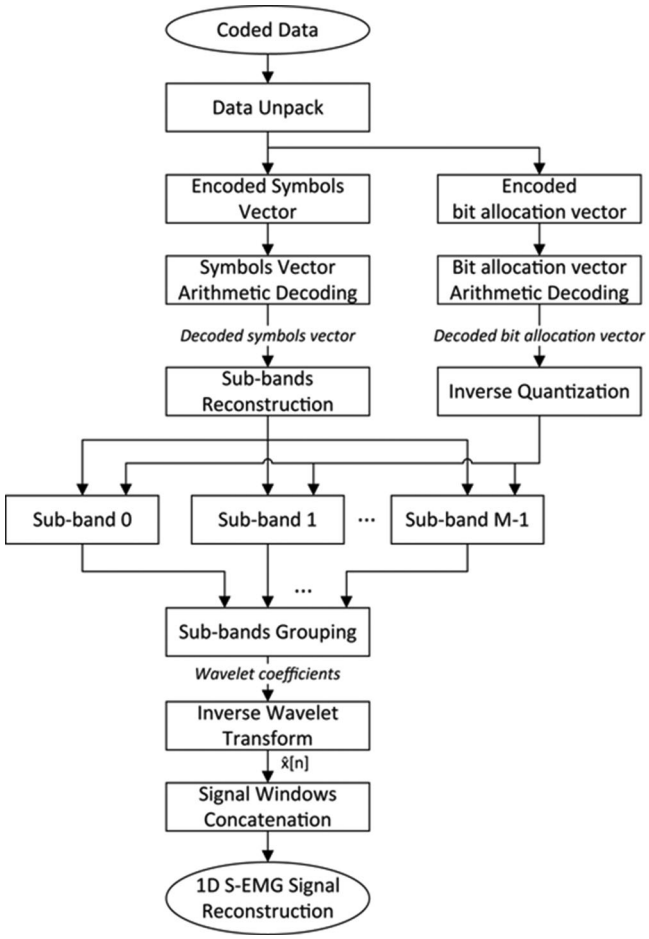

Fig. 2. Block diagram of 1D WDAL decoder.

After having computed the vector, $B[m]$, $\gamma[m]$ can be calculated in the form

$$\gamma[m] = 2^{B[m]} \tag{12}$$

$\gamma[m]$ is used in (2) to quantize the wavelet coefficients. The vector $B[m]$ (2) is compressed by an entropy encoder and packaged in the compress data file as lateral information to be used in the decoder to perform the inverse quantization.

After quantization, the sub-bands are regrouped to construct the symbol vector $W_q[k].W_q[k]$ and $B[m]$ are compressed by the arithmetic encoder [46], which has been shown to be more efficient compared to run-length and Huffman techniques. In the last step, the data is packaged generating the final compressed representation of the S-EMG signal.

B. 1D Algorithm Decoder

In the decoder, illustrated by the block diagram of Fig. 2, the data is unpacked. The lossless decoder is applied to obtain the symbols vector corresponding to the quantized coefficient vector and the vector $B[m]$. The sub-bands are reconstructed and then inverse quantization is performed. Next, the sub-bands are regrouped and the inverse wavelet transform is taken. Finally, the segments are concatenated in order to obtain the decoded S-EMG signal.

III. 2D S-EMG Signal Compression

To address the two-dimensional coding of S-EMG signals, we integrate the High Efficient Video Coding (HEVC) video encoder in the proposed algorithm. The HEVC [55]–[57], also known as H.265, is the state-of-the-art standard for video coding. It was developed by the Joint Collaborative Team on Video Coding (JCT-VC), which is form by the ITU-T Video Coding Experts Group (VCEG) and ISO/IEC Motion Picture Experts Group (MPEG). The first version of the standard was finalized in January 2013.

When compared to the previous standard H.264/AVC, HEVC can reduce the bit rate by 40% on average for a similar objective image quality (using Main Profile) [58], [59]. In order to do so, HEVC offers a series of encoding tools that can adapt to the data content. The basic encoding unit is the Coding Tree Unit (CTU), which is formed by luminance and chrominance image blocks. The CTU block scan have variable size from 64×64 to 8×8 pixels. An initial CTU size is set; and during encoding, the CTU will be partitioned up to its minimum size, if that yields better encoding performance. In each partition level, the CTU is coded using differential coding by inter- or intra-fame predictions. Intra-frame prediction means that each block is predicted from the pixels in the neighbor blocks, which have already been processed, according to a determined prediction mode, and only the quantized difference between the original signal and its prediction is encoded. HEVC offers up to 35 intra prediction modes. This is a significant increment of intra modes compare to previous standards [58]–[61]. During inter-frame prediction, the block is predicted from pixels belonging to previously encode frames. The reference frames can be past or future frames, if bi-prediction is used. Each CTU can be partitioned into Prediction Units (PUs), which can be symmetrical and non-symmetrical. After the PU is selected, the spatial redundancy is also reduced using Transform Coding. Discrete Cosine Transform is used for most blocks, while Discrete Sine Transform can be used in special cases for chrominance data. There are also different Transform sizes, which are referred to as Transform Units that vary from 4×4 to 32×32. Finally, an adaptive entropy encoder is used for both the motion information and the residual data. The entropy encoder is similar to the one used in H.264/AVC.

A previous work has also use HEVC in order to encode S-EMG signals; moreover, this work has also proposed a pre-processing step to better construct the 2D input signal [44]. However, the pre-processing step for the Dynamic Protocol presented here is novel, and it can generate spatial patterns that can be more efficiently encoded by the HEVC Intra mode. HEVC, as do most video encoders, uses fixed-point Discrete Transforms. In order to reduce the distortion introduced by the transformation, we setup HEVC to work with 16 bit-depth internal precision. We also ensure that the size of the input signal is large enough, so all CTU and PU sizes and prediction modes are available. This configuration enables HEVC to yield competitive results even with a simple pre-processing step as the one used for the Isometric Protocol. The pre-processing step and decoding algorithm for both protocols are detailed in the following sections.

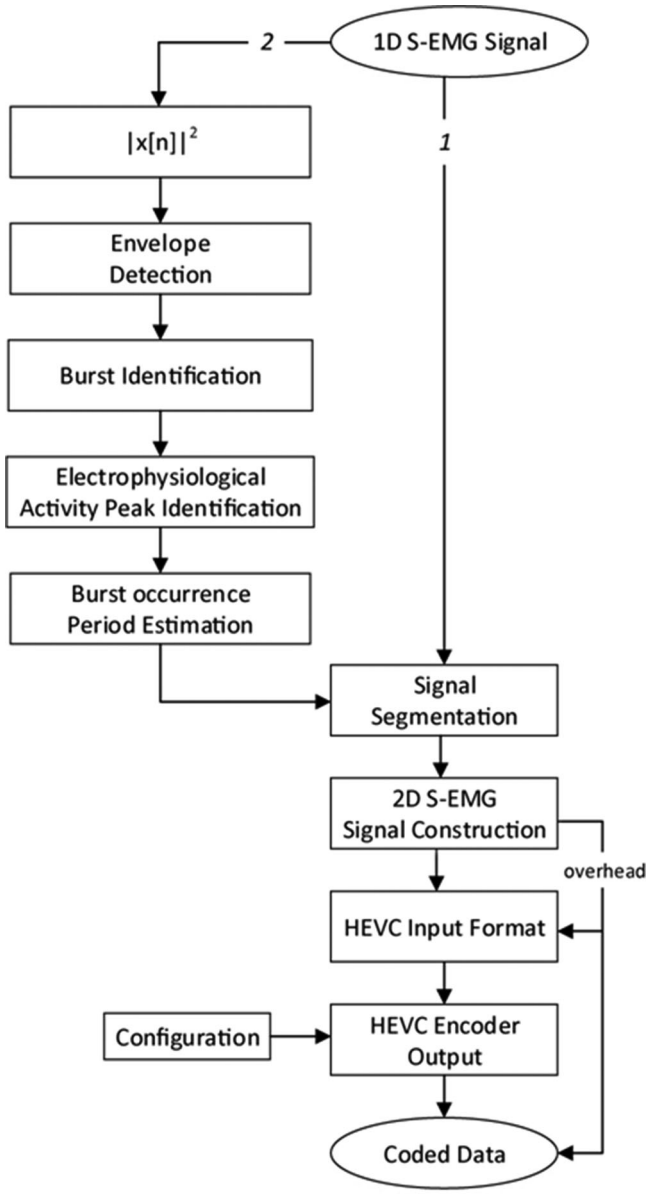

Fig. 3. Simplified block diagram of 2D BD–HEVC (2D Burst Detection HEVC) signal encoding of dynamic protocol.

A. 2D Encoder Algorithm Proposal for Dynamic Protocol

Fig. 3 shows a simplified diagram illustrating the independent modules that constitute the proposed 2D BD-HEVC (2D Burst Detection HEVC) methodology for encoding 2D S-EMG signals in dynamic experimental protocols. In the left branch of Fig. 3, the block diagram describes the procedures used for the S-EMG segmentation and 2D version signal construction. The absolute value of the S-EMG signal samples is taken and a low pass filtering is applied in order to obtain the signal envelope as shown in Fig. 4. The signal burst is identified and, at each

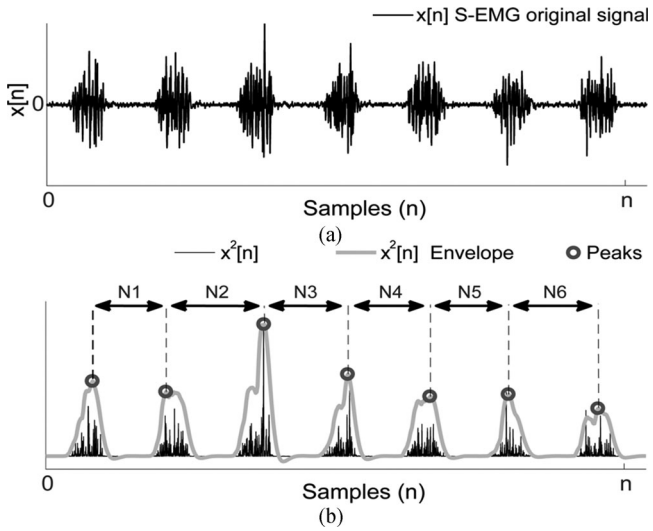

Fig. 4. (a) Dynamic S-EMG example and (b) burst estimation $N_i, i = 1, 2, \ldots$.

burst, the amplitude peak is detected. The computed temporal length in samples between successive bursts corresponds to an estimative occurrence interval. The physical experiment protocol is usually semi-periodic; therefore, the interval of occurrences between successive bursts is close to each other. The arithmetic mean is computed for all the intervals detected of burst occurrence, generating an estimative for the period of burst occurrence in samples.

The S-EMG signal is then segmented with segments of length equal to P samples, and arranged as different lines of a two-dimensional integer matrix. Each sample is represented by a 2-byte word length. The maximum and the minimum values are computed in the 2D S-EMG signal, and a DC value is added to build a 2D signal which has only positive values. This can be illustrated briefly by Fig. 5.

The next step, as shown in the block diagram of Fig. 3, is to apply the generated 2D signal [Fig. 5(b)] to the input of HEVC encoder, which on that occasion is configured with Monochrome 16 Intra profile. In this profile, the encoder will use the 4:0:0 image pattern (luminance samples only), word depth equal to 16 bits, and only the intra-frames prediction.

The proposed 2D array construction increases the spatial correlation between samples; therefore, intra-prediction will work efficiently. In this approach, the complete S-EMG signal is transform into just a single image. Furthermore, the *Deblocking Filter* (DBF), *Sample Adaptive Offset* (SAO) filters, and the *Conformance Window Mode* parameter are active, which enables block padding up to the minimum size of a CU [60], [61].

To the encoded data obtained as output from the HEVC encoder, overhead information about the dynamic range of the 1D S-EMG source signal is added. This information is necessary in the decoding process.

B. 2D Encoder Algorithm Proposal for Isometric Protocol

In the isometric protocol, the signal does not possess any burst. Therefore, the previously proposed method for construction of the 2D array can only be applied to the dynamic protocol. Nevertheless, a simpler 2D array can be created by using a fixed size for each row in the array. The fixed size can be set to the square root value of the original number of samples of the 1D signal. This will create a rectangular image (RI). If this value is not an integer number, then it can be rounded up and a zero padding is performed to complete the rectangular image. If this is the case, the number of zeros added to the signal is sent to the decoder as side-information.

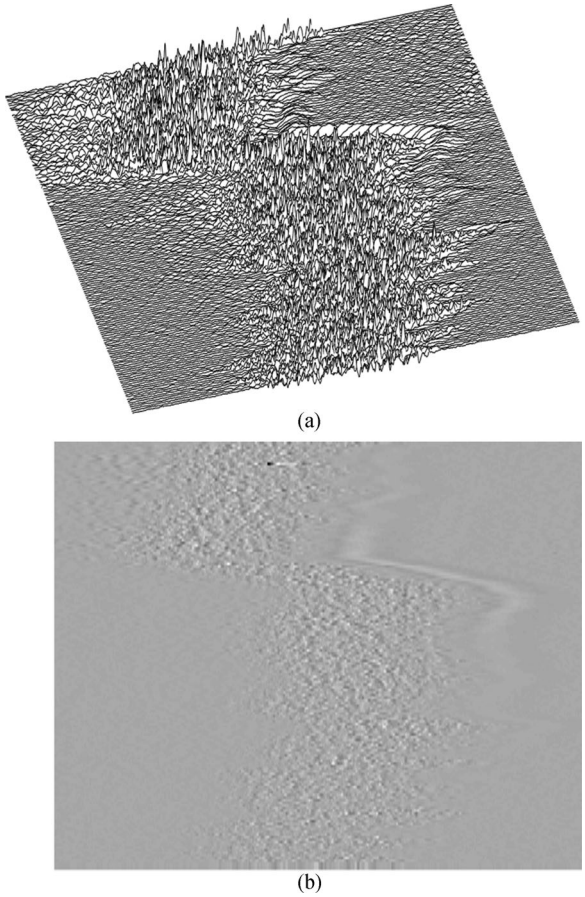

Fig. 5. 2D S-EMG signal construction example. (a) Segmented S-EMG signal amplitude in 3D representation. (b) 2D image final representation.

C. 2D Algorithm Decoder

In the decoding process, initially, the overhead information is taken from the packet data for future use in the S-EMG signal reconstruction, and the HEVC input format file is built. Fig. 6 shows the decoder block diagram. The output signal from the HEVC decoder is processed to match the dynamic range and DC level of the original S-EMG signal. Finally, 2D to 1D conversion is done by concatenating the lines of the 2D S-EMG signal.

IV. Evaluation Methods

The two metrics are most commonly used in scientific literature to evaluate the performance of the encoders: The Compression Factor (CF) and the Percent Residual Difference (PRD) [27], [29], [30], [32], [36]–[41], [44], [48]. The compression

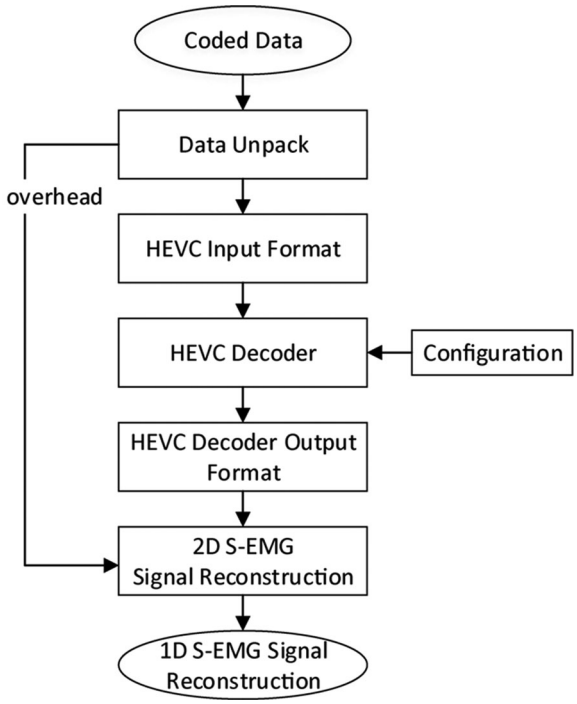

Fig. 6. Block diagram of 2D BD-HEVC (2D Burst Detection HEVC) for decoding of the dynamic protocol signal.

factor is defined by

$$CF\,(\%) = \frac{Os\ -\ Cs}{Os}\ 100 \tag{13}$$

where O_s is the number of bits required for storing the original data, and C_s is the number of bits to represent the compressed data. The PRD is defined as

$$PRD\,(\%) = \sqrt{\frac{\sum_{n=0}^{N-1}(x\,[n] - \hat{x}\,[n])^2}{\sum_{n=0}^{N-1} x[n]^2}} \tag{14}$$

where x is the original signal, $\hat{x}$ is the decoded signal, and N is the number of samples in the signal.

To evaluate and compare performances of the proposed encoders and the ones found in the scientific literature, two distinct experimental protocols were addressed: isometric protocol and dynamic protocol, as detailed below.

A. Isometric Protocol

In order to make a comparative performance evaluation of the proposed encoders with other works published in the literature, the same signal data bank was used as in [36], [37], [40], [44], and [48]. To build a signal data bank based on an experimental isometric protocol, pre-amplified surface electrodes (model DE-02, DelSys Inc. Boston MA, USA) were used. The location of the electrodes was chosen in order to obtain signals from the biceps brachii muscle. In the experiment, 14 subjects were submitted to a force intensity with production of muscular fatigue, maintaining 60% of their maximum voluntary contraction. The signals were digitized through a data acquisition card with LabVIEW (NI-DAQ for Windows, National Instruments, USA). All signals were sampled at 2000 Hz, quantized with 12 bits and stored in 16-bit digital words. The signal duration varied from 3 to 6 minutes.

B. Dynamic Protocol

To evaluate the proposed encoders in a dynamic protocol, a S-EMG signal data bank constructed by Andrade *et al.* [62] was used. A set of S-EMG signals collected from the vastus medialis muscle was used from 9 individuals riding a cycloergometer (Ergo-Fit, model Ergo Cycle 167, Pirmasens, Germany). In the experimental protocol, the speed was set at 30 km/h and a fixed load higher than 250 W was established. The S-EMG signals were transduced by pre-amplified surface electrodes (model DE-02, DelSys Inc., Boston, MA, USA), and digitalized by a data acquisition card with LabVIEW (NI-DAQ for Windows, National Instruments, USA). All signals were sampled at 2 kHz and quantized with 16 bits. The duration of the signals varied from 3 to 9 minutes.

In the next section, the results obtained are presented. Performance evaluations compared to other methods found in the literature are also shown.

V. Results

The 1D proposed algorithm will be referred to as 1D WDAL, while the 2D method based on burst detection for the dynamic protocol and the 2D rectangular image method will be called 2D BD-HEVC and 2D RI-HEVC, respectively. It is important to mention that one advantage of the 1D WDAL, is that it can be easily applied to both the isometric and dynamic protocols.

A. Results Using Isometric Protocol

To construct the two-dimensional signal used for the 2D RI-HEVC encoder (2D Rectangular Image HEVC) input, the S-EMG signal is first segmented into fixed 64-sample multiple windows. In the example shown in Fig. 7, a window length of 128 samples was chosen. The segments are arranged in order to construct a matrix for the two-dimensional signal representation. A DC value is finally added so that the amplitude of each sample assumes a positive value.

Fig. 7 shows the average result measuring PRD as a function of CF. The results show that the PRD rapidly increases when the CF is increased over 90%. Table I succinctly illustrates a comparative performance evaluation between the encoders for specific CF.

Results of the comparative evaluation for isometric protocol are summarized in Fig. 7 and Table I. For CF less than 75%, the 1D WDAL encoder presents better results for PRD. For CF between 75% and 85%, the HEVC encoder achieved the lowest PRD. For 90% CF, the results reported by Melo *et al.* [44], and for 95% CF, the results reported by Filho *et al.* [48] presented the lowest PRD values.

B. Results Using Dynamic Protocol

A summary of the PRD averaged results according to the CF for the S-EMG signal data bank used for dynamic experimental

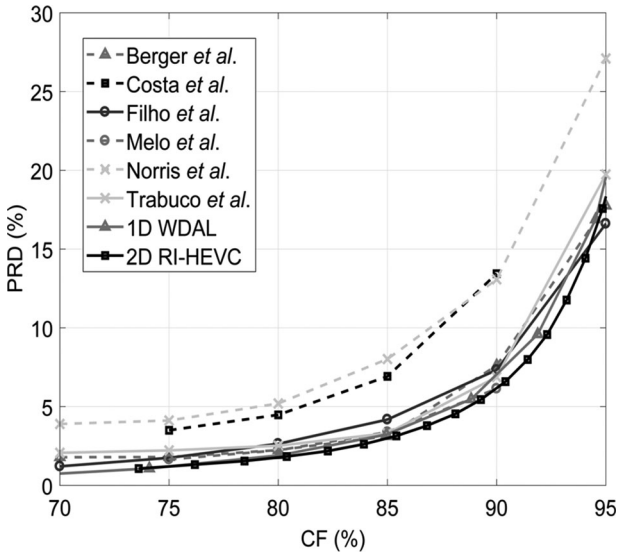

Fig. 7. Simulation results for isometric protocol. The proposed techniques are identified in figure: 1D WDAL (1D Wavelet Dynamic Adaptive Bit Allocation) and 2D RI-HEVC (2D Rectangular Image HEVC).

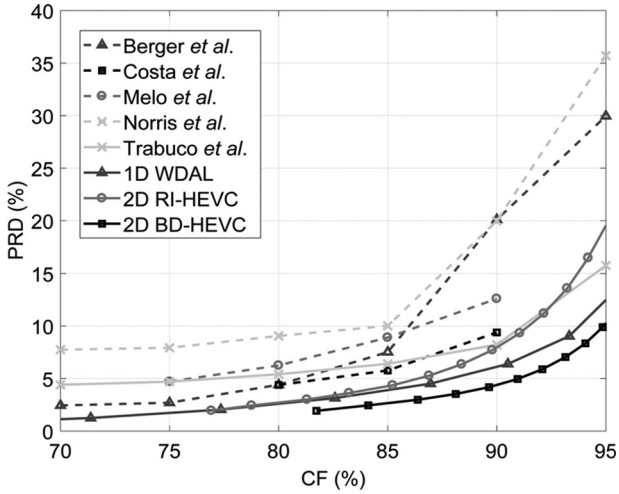

Fig. 8. Performance evaluations of encoders for dynamic protocol. The proposed techniques are identified in figure: 1D WDAL (1D Wavelet Dynamic Adaptive Bit Allocation) and 2D BD-HEVC (2D Burst Detection HEVC). The performance is also shown of the 2D RI-HEVC (2D Rectangular Image HEVC), in which the 2D S-EMG signal is constructed with fixed window segmentation as was implemented for the isometric protocol.

TABLE I
COMPARATIVE PERFORMANCE EVALUATION FOR ISOMETRIC PROTOCOL- PRD (%)

	Compression Factor - CF(%)					
	70	75	80	85	90	95
Berger *et al.* [37]	1.79	1.80	2.24	3.13	7.61	17.76
Costa *et al.* [40]	-	3.50	4.48	6.92	13.44	-
Filho *et al.* [48]	1.21	1.75	2.64	4.18	7.33	**16.61**
Melo *et al.* [44]	-	1.65	2.23	3.38	**6.14**	-
Norris *et al.* [30]	3.90	4.12	5.20	8.02	13.08	27.10
Trabuco *et al.* [36]	2.07	2.22	2.52	3.31	6.88	19.74
1D WDAL	**0.77**	1.24	1.99	3.36	7.06	19.28
2D RI-HEVC	-	**1.21**	**1.78**	**2.99**	6.18	18.33

Note: Best results in bold (lowest PRD for a given CF).

TABLE II
COMPARATIVE PERFORMANCE EVALUATION FOR DYNAMIC PROTOCOL- PRD (%)

	Compression Factor - CF(%)					
	70	75	80	85	90	95
Berger *et al.* [37]	2.44	2.70	4.41	7.52	20.10	29.96
Costa *et al.* [40]	-	-	4.39	5.77	9.39	-
Melo *et al.* [44]	-	4.71	6.25	8.91	12.60	-
Norris *et al.* [40]	7.75	7.93	9.06	10.02	19.98	35.71
Trabuco *et al.* [36]	4.41	4.70	5.41	6.40	8.22	15.76
1D WDAL	**1.12**	**1.74**	**2.64**	3.93	6.11	12.63
2D RI-HEVC	-	-	2.71	4.28	7.96	19.53
2D BD-HEVC	-	-	-	**2.66**	**4.39**	**10.28**

Note: Best results in bold (lowest PRD for a given CF).

protocol is shown in Fig. 8. Table II presents a comparative evaluation for specific CF.

The panoramic view in Fig. 8 shows the performance evaluation of the various encoders for dynamic experimental protocol. Table II summarizes the results found of the percent residual difference (PRD) for specific value of CF. The proposed 1D WDAL encoder has better performance compared to the other techniques reported in Table II for CF equal or below 80%. On the other hand, the proposed 2D BD-HEVC encoder presented the lowest PRD when CF is equal or higher than 85%.

According to results of the presented simulations shown in Fig. 8, the 2D S-EMG constructed using the burst peak segmentation improves the encoder performance. In the experimental dynamic protocol, the 2D Burst-Detection HEVC (2D BD-HEVC) encoder presents better compression results for the same CF compared to the 2D Rectangular Image HEVC (2D RI-HEVC) encoder.

VI. DISCUSSION

The results show that the proposed technique can outperform previous works found in the literature. The 2D encoder provides better results for high compression rates. This is expected since the HEVC has been reported to outperform its predecessor image/video encoders for high compression rates [55], [56]. In addition to presenting superior performance when compared to other efficient S-EMG coding techniques found in the literature, the HEVC encoder is a commercial off-the-shelf product available on several platforms.

During the segmentation algorithm of dynamic S-EMG signals, the bursts are positioned side by side for construction of the 2D signal version. In dynamic S-EMG signals during the segmentation algorithm, the bursts are positioned side by side for construction of the 2D signal version. This approach allows the creation of regions with similar spatial patterns, which can be exploited by the Intra modes of the HEVC. Moreover, it

is observed that some regions possess a small variation of the dynamic range, while others have a large variation (as can be seen in Fig. 5). Therefore, the use of internal 16 bit-depth precision is critical for the S-EMG signal, since this increases the dynamic range of the encoder during internal operations. This is in accordance with previous evaluation tests of the HEVC encoder [55]–[57].

The pre-processing method used to construct the 2D input signal does not prevent the encoder and decoder to be compliant with the H.265 standard. While the 1D encoder presents worse performance compared to the 2D encoder at high compression rates, it presents better performance at low compression rates. This is mostly evident for the dynamic signals encoding as shown in Fig. 8 and Table II. This is due to mainly two issues.

First, at low compression rates HEVC uses low quantization steps. This is not a major issue for natural still images because pixels are normally highly correlated. However, S-EMG signal can resemble noise, and the use of a low quantization parameter can reduce the efficiency of the spatial differential pulse code modulation of Intra encoding. Second, the proposed 1D technique has a bit allocation that adapts to the signal characteristics. Its superior performance for low-compression rates is achieved by allocating a larger number of bits for the coefficient vector quantization of the wavelet transform. The 1D proposed compression methodology also has the advantage that it can yield competitive results using the same procedure for both Isometric and Dynamic signals, while a different pre-processing step is required for the 2D encoder.

Despite the good performance, it is also important to note that our proposals have some limitations. In order for the HECV encoder to have access to all its coding tools, e.g., all intra-prediction modules [55], the constructed 2D input signals from isometric and dynamic S-EMG 1D signals need a number of rows and columns greater than 64×64. In the case of signals obtained in dynamic experimental protocols, it means that the signal must have at least 65 bursts so that the 2D version built by the segmentation meets the requirements for full utilization of the HEVC encoder resources.

VII. Conclusion

In this work, two techniques for S-EMG signal encoding were developed for dynamic experimental protocols. Furthermore, the proposed techniques also presented good performance for isometric experimental protocols. The proposed 1D WDAL technique performed well. In the isometric protocol for CF less than 75% and in the dynamic protocol for CF less than 85%, it presented the best results. On the other hand, the proposed 2D BD-HEVC technique efficiently segmented the S-EMG signal based on a burst peak detection, which makes appropriately sorting the segments to construct a 2D signal possible. Comparison of the results between RI-HEVC and BD-HEVC indicated the efficiency of proposed S-EMG signal segmentation. In the dynamic protocol, for high levels of CF (greater than 80%), the BD-HEVC technique presented the best performance.

The proposed 1D and 2D coders were very efficient for encoding S-EMG signals. The continuity of the research points towards a comparative performance evaluation from S-EMG signals collected on other muscles and a comparative performance evaluation with other experimental protocols. Also, a new study of an improvement of pre-processing step specifically design to use with HEVC for the isometric and dynamic protocols can be the focus of future researches.

References

[1] T. Kamali, R. Boostani, and H. Parsaei, "A multi-classifier approach to MUAP classification for diagnosis of neuromuscular disorders," *IEEE Trans. Neural Syst. Rehabil. Eng.*, vol. 22, no. 1, pp. 191–200, Jan. 2014, doi: 10.1109/TNSRE.2013.2291322.

[2] A. B. M. S. U. Doulah, S. A. Fattah, W. -P. Zhu, and M. O. Ahmad, "Wavelet domain feature extraction scheme based on dominant motor unit action potential of EMG signal for neuromuscular disease classification," *IEEE Trans. Biomed. Circuits Syst.*, vol. 8, no. 2, pp. 155–164, Apr. 2014, doi: 10.1109/TBCAS.2014.2309252.

[3] S. Baudry, M. A. Minetto, and J. Duchateau, "Surface EMG applications in neurophysiology," in *Surface Electromyography: Physiology, Engineering, and Applications*, R. Merletti and D. Farina, Eds. Hoboken, NJ, USA: Wiley, 2016, pp. 333–360.

[4] A. Rainoldi, T. Moritani, and G. Boccia, "EMG in exercise physiology and sports," in *Surface Electromyography: Physiology, Engineering, and Applications*, R. Merletti and D. Farina, Eds., Hoboken, NJ, USA: Wiley, 2016, pp. 501–539.

[5] A. Aliverti *et al.*, "Functional evaluation and rehabilitation engineering," *IEEE Pulse*, vol. 2, no. 3, pp. 24–34, May/Jun. 2011, doi: 10.1109/MPUL.2011.941520.

[6] C. Wong, Z. Zhang, Benny Lo, and G. Yang, "Wearable sensing for solid biomechanics: A review," *IEEE Sensors J.*, vol. 15, no. 5, pp. 2747–2760, May 2015, doi: 10.1109/JSEN.2015.2393883.

[7] J. L. Segil, S. A. Huddle, and R. F. Weir, "Functional assessment of a myoelectric postural controller and multi-functional prosthetic hand by persons with trans-radial limb loss," *IEEE Trans. Neural Syst. Rehabil. Eng.*, vol. 25, no. 6, pp. 618–627, Jun. 2017, doi: 10.1109/TNSRE.2016.2586846.

[8] W. Guo, X. Sheng, H. Liu, and X. Zhu, "Mechanomyography assisted myoeletric sensing for upper-extremity prostheses: A hybrid approach," *IEEE Sensors J.*, vol. 17, no. 10, pp. 3100–3108, Mar. 2017, doi: 10.1109/JSEN.2017.2679806.

[9] A. P. Guerrero and C. Mailhes, "On the choice of an electromyogram data compression method," in *Proc. 19th IEEE Int. Conf. Eng. Med. Biol. Soc.*, Chicago, IL, USA, 1997, vol. 4, pp. 1558–1561.

[10] E. S. G. Carotti, J. C. De Martin, D. Farina, and R. Merletti, "Linear predictive coding of myoelectric signals," in *Proc. IEEE Int. Conf. Acoust., Speech, Signal Process.*, Philadelphia, PA, USA, 2005, vol. 5, pp. 629–632.

[11] E. S. G. Carotti, J. C. De Martin, R. Merletti, and D. Farina, "Compression of surface EMG signals with algebraic code excited linear prediction," in *Proc. IEEE Int. Conf. Acoust., Speech, Signal Process.*, Toulouse, France, 2006, vol. 3, pp. 1148–1151.

[12] E. S. G. Carotti, J. C. De Martin, R. Merletti, and D. Farina, "ACELP-based compression of multi-channel surface EMG signals," in *Proc. IEEE Int. Conf. Acoust., Speech, Signal Process.*, Honolulu, HI, USA, 2007, vol. 2, pp. 361–364.

[13] E. S. G. Carotti, J. C. De Martin, R. Merletti, and D. Farina, "Matrix-based linear predictive compression of multi-channel surface," in *Proc. IEEE Int. Conf. Acoust., Speech, Signal Process.*, Las Vegas, NV, USA, 2008, pp. 493–496.

[14] E. S. G. Carotti, J. C. De Martin, R. Merletti, and D. Farina, "Compression of multidimensional biomedical signals with spatial and temporal codebook-excited linear prediction," *IEEE Trans. Biomed. Eng.*, vol. 56, no. 11, pp. 2604–2610, Jul. 2009, doi: 10.1109/TBME.2009.2027691.

[15] A. S. Spanias, "Speech coding: A tutorial review," *Proc. IEEE*, vol. 82, no. 10, pp. 1541–1582, Oct. 1994, doi: 10.1109/5.326413.

[16] R. Salami *et al.*, "Design and description of CS-ACELP: A toll quality 8 kb/s speech coder," *IEEE Trans. Speech Audio Process.*, vol. 6, no. 2, pp. 116–130, Mar. 1998, doi: 10.1109/89.661471.

[17] H. W. Adelmann, Y. C. Ching, and B. Gotz, "An ADPCM approach to reduce the bit rate of μ-law encoded speech," *Bell Syst. Tech. J.*, vol. 58, pp. 1659–1671, Sep. 1979, doi: 10.1002/j.1538-7305.1979.tb02275.x.

[18] D. Goodman, "Embedded DPCM for variable bit rate transmission," *IEEE Trans. Commun.*, vol. 28, no. 7, pp. 1040–1046, Jul. 1980, doi: 10.1109/TCOM.1980.1094764.

[19] J. F. Norris and D. F. Lovely, "Real-time compression of myoelectric data utilising adaptive differential pulse code modulation," *Med. Biol. Eng. Comput.*, vol. 33, no. 5, pp. 629–635, Sep. 1995, doi: 10.1007/BF02510779.

[20] A. D. C. Chan, D. F. Lovely, and B. Hudgins, "Errors associated with the use of adaptive differential pulse code modulation in the compression of isometric and dynamic myo-electric signals," *Med. Biol. Eng. Comput.*, vol. 36, no. 2, pp. 215–219, Mar. 1998, doi: 10.1007/BF02510745.

[21] A. Yousefian, S. Roy, and B. Gosselin, "A low-power wireless multichannel surface EMG sensor with simplified ADPCM data compression," in *Proc. 2013 IEEE Int. Symp. Circuits Syst.*, Beijing, China, 2013, pp. 2287–2290.

[22] S. Sharma and M. Singh, "On board EMG signal compression for portable devices—A study," in *Proc. Int. Conf. Mach. Intell. Res. Adv.*, Katra, India, 2013, pp. 584–588.

[23] Y. Linde, A. Buzo, and R. M. Gray, "An algorithm for vector quantizer design," *IEEE Trans. Commun.*, vol. 28, no. 1, pp. 84–95, Jan. 1980, doi: 10.1109/TCOM.1980.1094577.

[24] T. K. Grönfors and N. S. Päivinen, "Comparison of vector quantization methods for medical fidelity preserving lossy compression of EMG signals," in *Proc. Int. Conf. Comput. Intell. Modell, Control Autom.*, Vienna, Austria, 2005, pp. 1107–1113.

[25] T. K. Grönfors and N. S. Päivinen, "The effect of vector length and gain quantization level on medical parameters of EMG signals on lossy compression," in *Proc. IET 3rd Int. Conf. Adv. Med., Signal Inf. Process.*, Glasgow, U.K., 2006, pp. 1–4.

[26] T. Grönfors, M. Reinikainen, and T. Sihvonen, "Vector quantization as a method for integer EMG signal compression," *J. Med. Eng. Technol.*, vol. 30, no. 1, pp. 41–52, Jan./Feb. 2006, doi: 10.1080/03091900500130872.

[27] P. A. Berger, F. A. O. Nascimento, J. C. Carmo, A. F. Rocha, and I. dos Santos, "Algorithm for compression of EMG signals," in *Proc. 25th IEEE Int. Conf. Eng. Med. Biol. Soc.*, Cancun, Mexico, 2003, vol. 2, pp. 1299–1302.

[28] P. Wellig, Z. Cheng, M. Semling, and G. S. Moschytz, "Electromyogram data compression using single-tree and modified zero-tree wavelet encoding," in *Proc. 20th IEEE Int. Conf. Eng. Med. Biol. Soc.*, Hong Kong, China, 1998, vol. 3, pp. 1303–1306.

[29] J. A. Norris, K. Englehart, and D. Lovely, "Steady-state and dynamic myoelectric signal compression using embedded zero-tree wavelets," in *Proc. 23rd IEEE Int. Conf. Eng. Med. Biol. Soc.*, Istanbul, Turkey, 2001, vol. 2, pp. 1879–1882.

[30] J. A. Norris, K. B. Englehart, and D. F Lovely, "Myoelectric signal compression using zero-trees of wavelet coefficients," *Med. Eng. Phys.*, vol. 25, no. 9, pp. 739–746, Nov. 2003, doi: 10.1016/S1350-4533(03)00118-8.

[31] L. Brechet, M. F. Lucas, C. Doncarli, and D. Farina, "Compression of biomedical signals with mother wavelet optimization and best-basis wavelet packet selection," *IEEE Trans. Biomed. Eng.*, vol. 54, no. 12, pp. 2186–2192, Dec. 2007, doi: 10.1109/TBME.2007.896596.

[32] J. P. L. M. Paiva, C. A. Kelencz, H. M. Paiva, R. K. H. Galvão, and M. Magini, "Adaptive wavelet EMG compression based on local optimization of filter banks," *Physiol. Meas.* vol. 29, no. 7, pp. 843–856, Jul. 2008, doi: 10.1088/0967-3334/29/7/012.

[33] A. J. Oyobé-Okassa and P. Elé, "Optimization of the compression ratio of the modified algorithm of decomposition electromyographic signals by a superimposed coding," in *Proc. 10th Int. Conf. Signal-Image Technol. Internet-Based Syst.*, Marrakech, Morocco, 2014, pp. 83–93.

[34] S. Sarkar and A. K. Bhoi, "Compression of surface electromyographic signal using wavelet packet 1D," *Int. J. Pharmaceutical Sci . Health Care*, vol. 4, no. 2, pp. 115–121, Aug. 2012.

[35] N. Jain and R. Vig, "Wavelet based vector quantization with tree code vectors for EMG Signal compression," in *Proc. 6th WSEAS Int. Conf. Signal Process.*, Dallas, TX, USA, 2007, vol. 6, pp. 117–124.

[36] M. H. Trabuco, M. V. C. Costa, and F. A. O. Nascimento, "S-EMG signal compression based on domain transformation and spectral shape dynamic bit allocation," *BioMed. Eng. OnLine*, vol. 13, no. 1, pp. 13–22, 2014, doi: 10.1186/1475-925X-13-22.

[37] P. A. Berger, F. A. O. Nascimento, J. C. Carmo, and A. F. Rocha, "Compression of EMG signals with wavelet transform and artificial neural networks," *Physiol. Meas.*, vol. 27, no. 6, pp. 457–65, Jun. 2006, doi: 10.1088/0967-3334/27/6/003.

[38] P. A. Berger, F. A. O. Nascimento, A. F. Rocha, and J. L. A. Carvalho, "A new wavelet-based algorithm for compression of EMG signals," in *Proc. 29th IEEE Int. Conf. Eng. Med. Biol. Soc.*, Lyon, France, 2007, pp. 1554–1557.

[39] M. V. C. Costa, P. A. Berger, A. F. Rocha, J. L. A. Carvalho, and F. A. O. Nascimento, "Compression of electromyographic signals using image compression techniques," in *Proc. 30th IEEE Int. Conf. Eng. Med. Biol. Soc.*, Vancouver, BC, Canada, 2008, pp. 2948–2951.

[40] M. V. C. Costa, J. L. A. Carvalho, P. A. Berger, A. Zaghetto, A. F. Rocha, and F. A. O. Nascimento, "Two-dimensional compression of surface electromyographic signals using column-correlation sorting and image encoders," in *Proc. 31st IEEE Int. Conf. Eng. Med. Biol. Soc.*, Minneapolis, MN, USA, 2009, pp. 428–431.

[41] W. C. Melo, E. B. L. Filho, and W. S. S. Júnior, "Electromyographic signal compression based on preprocessing techniques," in *Proc. 34th IEEE Int. Conf. Eng. Med. Biol. Soc.*, San Diego, CA, USA, 2012, pp. 5404–5407.

[42] N. E. Pascal, P. Ele, S. Z. Dieudonné, and E. Tonye, "Evaluation of EMG signals compression by JPEG 2000 called 1D," *Int. J. Eng. Technol.*, vol. 5, no. 1, pp. 44–51, Feb.–Mar. 2013.

[43] N. E. Pascal, P. Ele, and K. I. Basile, "Compression approach of EMG signal using 2D discrete wavelet and cosine transforms," *Amer. J. Signal Process.*, vol. 3, no. 1, pp. 10–16, 2013, doi: 10.5923/j.ajsp.20130301.02.

[44] W. C. Melo, E. B. L. Filho, and W. S. S. Júnior, "SEMG signal compression based on two-dimensional techniques," *BioMed. Eng. OnLine*, vol. 15, no. 41, pp. 1–31, 2016, doi: 10.1186/s12938-016-0158-1.

[45] N. E. Pascal, T. M. Lionel, P. Ele, and K. I. Basile, "EMG signal compression using 2D fractal," *Int. J. Adv. Technol. Eng. Res.*, vol. 3, no. 3, pp. 58–68, May 2013.

[46] C. Itiki, S. S. Furuie, and R. Merletti, "Compression of high-density EMG signals for trapezius and gastrocnemius muscles," *BioMed. Eng. OnLine*, vol. 13, no. 25, pp. 1–23, Mar. 2014, doi: 10.1186/1475-925X-13-25.

[47] M. B. de Carvalho, E. A. B. da Silva, and W. A. Finamore, "Multidimensional signal compression using multiscale recurrent patterns," *Signal Process.*, vol. 82, no. 11, pp. 1559–1580, Nov. 2002, doi: 10.1016/S0165-1684(02)00302-X.

[48] E. B. L. Filho, E. A. B. Silva, and M. B. Carvalho, "On EMG signal compression with recurrent patterns," *IEEE Trans. Biomed. Eng.*, vol. 55, no. 7, pp. 1920–1923, Jul. 2008, doi: 10.1109/TBME.2008.919729.

[49] A. Salman, E. G. Allstot, A. Y. Chen, A. M. R. Dixon, D. Gangopadhyay, and D. J. Allstot, "Compressive sampling of EMG bio-signals," in *Proc. IEEE Int. Symp. Circuits Syst.*, Rio de Janeiro, Brazil, 2011, pp. 2095–2098.

[50] E. G. Allstot, A. Y. Chen, A. M. R. Dixon, D. Gangopadhyay, H. Mitsuda, and D. J. Allstot, "Compressed sensing of ECG bio-signals using one-bit measurement matrices," in *Proc. IEEE 9th Int. New Circuits Syst. Conf.*, Bordeaux, France, 2011, pp. 213–216.

[51] A. M. R. Dixon, E. G. Allstot, D. Gangopadhyay, and D. J. Allstot, "Compressed sensing system considerations for ECG and EMG wireless biosensors," *IEEE Trans. Biomed. Circuits Syst.*, vol. 6, no. 2, pp. 156–166, Apr. 2012, doi: 10.1109/TBCAS.2012.2193668.

[52] Y.-S. Chen, H.-Y. Lin, H.-C. Chiu, and H.-P. Ma, "A compressive sensing framework for electromyogram and electroencephalogram," in *Proc. IEEE Int. Symp. Med. Meas. Appl.*, Lisboa, Portugal, 2014, pp. 1–6.

[53] A. Ravelomanantsoa, H. Rabah, and A. Rouane, "Compressed sensing: A simple deterministic measurement matrix and a fast recovery algorithm," *IEEE Trans. Instrum. Meas.*, vol. 64, no. 12, pp. 3405–3413, Dec. 2015, doi: 10.1109/TIM.2015.2459471.

[54] I. H. Witten, R. M Neal, and J. G. Cleary, "Arithmetic coding for data compression," *Commun. ACM*, vol. 30, no. 6, pp. 520–540, Jun. 1987, doi: 10.1145/214762.214771.

[55] G. J. Sullivan, J.-R. Ohm, W.-J. Han, and T. Wiegand, "Overview of the high efficiency video coding (HEVC) standard," *IEEE Trans. Circuits Syst. Video Technol.*, vol. 22, no. 12, pp. 1649–1668, Dec. 2012, doi: 10.1109/TCSVT.2012.2221191.

[56] T. K. Tan *et al.*, "Video quality evaluation methodology and verification testing of HEVC compression performance," *IEEE Trans. Circuits Syst. Video Technol.*, vol. 26, no. 1, pp. 76–90, Jan. 2016, doi: 10.1109/TCSVT.2015.2477916.

[57] J. Vanne, M. Viitanen, T. D. Hamalainen, and A. Hallapuro, "Comparative rate-distortion-complexity analysis of HEVC and AVC video codecs," *IEEE Trans. Circuits Syst. Video Technol.*, vol. 22, no. 12, pp. 1885–1898, Dec. 2012, doi: 10.1109/TCSVT.2012.2223013.

[58] G. Tech, Y. Chen, K. Müller, J.-R. Ohm, A. Vetro, and Y.-K. Wang, "Overview of the multiview and 3D extensions of high efficiency video coding," *IEEE Trans. Circuits Syst. Video Technol.*, vol. 26, no. 1, pp. 35–49, Jan. 2016, doi: 10.1109/TCSVT.2015.2477935.

[59] D. Flynn *et al.*, "Overview of the range extensions for the HEVC standard: Tools, profiles, and performance," *IEEE Trans. Circuits Syst. Video Technol.*, vol. 26, no. 1, pp. 4–19, Jan. 2016, doi: 10.1109/TCSVT.2015.2478707.

[60] J. Xu, R. Joshi, and R. A. Cohen, "Overview of the emerging HEVC screen content coding extension," *IEEE Trans. Circuits Syst. Video Technol.*, vol. 26, no. 1, pp. 50–62, Jan. 2016, doi: 10.1109/TCSVT.2015.2478706.

[61] G. J. Sullivan, J. M. Boyce, Y. Chen, J.-R. Ohm, C. A. Segall, and A. Vetro, "Standardized extensions of high efficiency video coding," *IEEE J. Sel. Topics. Signal Process.*, vol. 7, no. 6, pp. 1001–1016, Dec. 2013, doi: 10.1109/JSTSP.2013.2283657.

[62] M. M. Andrade *et al.*, "Evaluation of techniques for the study of electromyographic signals," in *Proc. 28th IEEE Int. Conf. Eng. Med. Biol. Soc.*, New York, NY, USA, Sep. 2006, pp. 1335–1338.